NUMERICAL SIMULATION OF FEEDSTOCK MELT FILLING IN A CYLINDRICAL CAVITY WITH SOLIDIFICATION IN POWDER INJECTION MOLDING①

Qu Xuanhui, Li Yimin, Yue Hongsheng, Mao Jinying, Zhu Lei and Huang Baiyun
State Key Laboratory for Powder Metallurgy,
Central South University of Technology, Changsha 410083, P. R. China

ABSTRACT The solidification of wax-based Fe-2% Ni feedstocks melt on the wall of a cylindrical cavity during injection filling was simulated with a finite difference analysis method. The effects of injection molding paramaters on the solid layer profiles were studied. The results show that the frozen layer grows rapidly at the beginning but much lower after a critical thickness of solid layer forms. The thickness of frozen layer decreases with the increase of volume flow rate(injection speed) and wall temperature(die temperature). By comparing the computing results of inlet pressure(injection pressure) at different volume flow rates with and without frozen layers, it is predicted that higher injection pressure might be required to fill the cavity when the solidification is taken into consideration.

Key words powder injection molding numerical simulation solidification

1 INTRODUCTION

Powder injection molding(PIM) is a processing route for fabricating metal or ceramic components with complex shape and high performance at low cost. In this process, the metal or ceramic powders are mixed with a binder to produce a feedstock. Then, feedstock melts are filled into a closed cavity by injection molding to form a compact. The binder is extracted by a thermal or chemical process and the powder compact is sintered to a final density[1, 2].

The flow of feedstock melt is a transient, non-isothermal and non-Newtonian process with frozen layer building up on the wall as the fluid flows through the mold cavity. The transient melt with metal powder, compared with pure plastic, may result in rather thick frozen solid layer thus changing the flow cross section area of the cavity. It is referred to as a moving boundary problem[3] because the location of solid/liquid interface changes with time. Generally, this problem is difficult to solve. It is not only because of the two thermal boundary conditions at the interface, but also because the interface is not normally straight and it is constantly moving. Furthermore, the existence of temperature dependent material properties makes the mathematical treatment of such problem even more complex. Therefore, numerical methods are commonly adopted and simplification are inevitably used[4, 5].

The problem of solidification of a power-law feedstock melt flowing in a cylindrical mold cavity was investigated. To facilitate the finite difference numerical method coordinate transformation and trial-and-error method were employed to straighten and obtain the moving, curved solid/liquid interface. The effects of the processing parameters such as volume flow rate, injection temperature and the wall temperature on the profile of frozen layer were also determined. The computing results for the situation that solidification is considered were compared with that of no solidification considered. Two special boundary conditions regarding the energy balance were

① Received Jun. 16, 1998; accepted Aug. 8, 1998

specified at the solid/melt interface.

2 THEORY

As shown in Fig. 1, an incompressible fluid flows with constant property into a cold empty mold cavity and the flow is laminar. Both the mold wall temperature (T_w) and freezing temperature(T_s) of the melt which is well above T_w, keep constant during the mold filling process. The temperature at the entrance is uniform and equals the injection temperature(T_0). A frozen layer forms on the die wall after the fluid enters the cavity and its thickness increases with time while the flow front goes forward in the mold.

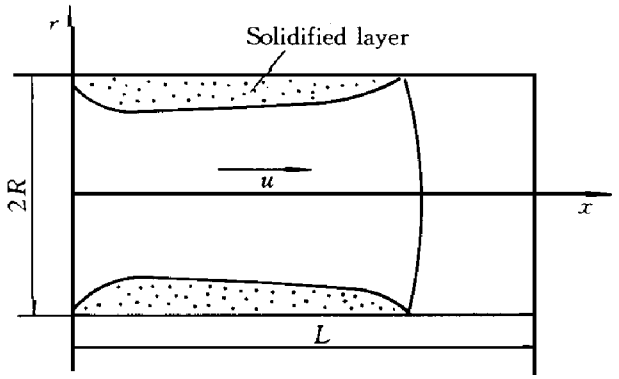

Fig. 1 A flow model of feedstock melt in a cylindrical mold cavity with solidification

Several assumptions are employed in this study to simplify the formulation.

1) The feedstock is homogeneous and its physical properties (ρ, C_p, λ) are time and temperature independent. The volume flow rate (Q) at the entrance keeps constant.

2) Both the solid and melt temperature along the solid/liquid boundary equal the freezing temperature of the feedstock material. The rate of heat transfer by conduction in both phases is equal at the interface since the solidification is at steady state.

3) Heat conduction along the flow direction of liquid is neglected. The solid layer thickness is much smaller than the flow length and the dominant direction of temperature gradient is in the radial direction.

4) Non-slip boundary condition is applied to the solid/liquid interface.

5) The radial velocity component is very small and the radial component of the equation of motion can be neglected.

6) The flow is fully developed and the fountain region in the vicinity of the advancing melt front is neglected. However, the temperature distribution along the new flow front is taken to be uniform and equal to the centerline temperature at the nearest upstream melt to mimic the "fountain" which allows hot feedstock to flow from the center of the mold to the cold wall.

A powder-law rheology model is employed in this study:

$$\eta = m_0 \exp(T_a/T)\dot{\gamma}^{n-1} \tag{1}$$

where T denotes temperature, n is power-law index, m_0 and T_a are material dependent constants, η is shear viscosity and $\dot{\gamma}$ is shear rate ($= \left|\frac{\partial u}{\partial r}\right|$, u is velocity).

The governing equations of the momentum and energy balance for the feedstock melt are described as

$$\frac{\partial p}{\partial x} = \frac{1}{r}\frac{\partial}{\partial r}\left(r\eta\frac{\partial u}{\partial r}\right) \tag{2}$$

$$\rho C_p\left(\frac{\partial T}{\partial t} + u\frac{\partial T}{\partial x}\right) = \frac{\lambda}{r}\frac{\partial T}{\partial r} + \lambda\frac{\partial^2 T}{\partial r^2} + \eta\dot{\gamma}^2 \tag{3}$$

where p is pressure, ρ is density, C_p is thermal capacity, λ is heat conductivity and t denotes time.

Furthermore, global conservation of mass states that

$$Q = 2\pi\int_0^{R-g(x)} ru\,dr \tag{4}$$

where $g(x)$ is the thickness of solid layer which is space and time dependent.

In the solid phase, the energy equation is given by

$$\rho C_p\frac{\partial T}{\partial t} = \frac{\lambda}{r}\frac{\partial T}{\partial r} + \lambda\frac{\partial^2 T}{\partial r^2} \tag{5}$$

The corresponding initial and boundary conditions of temperature, velocity, pressure and interface location are described as follows:

$T = T_0$ at the entrance ($x = 0$); $T = T_W$ at the wall ($r = R$);

$T = T_s$, $u = 0$, $\left|\frac{\partial T}{\partial r}\right|_s = \left|\frac{\partial T}{\partial r}\right|_l$ at the solid/liquid interface ($r = \delta(x)$); (6)

$\frac{\partial T}{\partial r} = 0$, $\frac{\partial u}{\partial r} = 0$ at the centerline ($r = 0$);

$p = 0$ at the melt front.

$\left|\frac{\partial T}{\partial r}\right|_s$ and $\left|\frac{\partial T}{\partial r}\right|_l$ denote the temperature gradient at the moving boundary for solid and liquid phases, respectively.

By integrating the momentum equation, making use of the aforementioned boundary conditions for velocity as well as the mass conservation equation and the power-law rheology equation, the pressure gradient, velocity and shear rate profiles for the liquid can be obtained as

$$\frac{\partial p}{\partial x} = -\left|\frac{Q}{\pi\int_0^{\delta(x)} r^2\left[\frac{nd}{2m_0\exp(T_a/T)}\right]^{1/n}\mathrm{d}r}\right|^n \quad (7)$$

$$u = \int_r^{\delta(x)}\left|\frac{\left|\frac{\partial p}{\partial x}\right| r}{2m_0\exp(T_a/T)}\right|^{1/n}\mathrm{d}r \quad fr \quad (8)$$

$$\dot{\gamma} = \left|\frac{\partial u}{\partial r}\right| = \left|\frac{\left|\frac{\partial p}{\partial x}\right| r}{2m_0\exp(T_a/T)}\right|^{1/n} \quad (9)$$

where $\delta(x) = R - g(x)$

3 NUMERICAL SOLUTION

Because no analytical solutions are available, a fully implicit finite difference numerical method[8, 9] was applied to the energy governing equations. To make the implementation of the finite difference method conveniently, coordinate transformations[8] are employed to straighten and immobilize the boundary. New coordinate variables $y(x)$ and $z(x)$ are introduced into the model and the definitions are given by

$$y(x) = \frac{r}{\delta(x)} \text{ (in the liquid region)} \quad (10)$$

$$z(x) = \frac{r - \delta(x)}{\delta(x)} \text{ (in the solid region)} \quad (11)$$

where the value of $y(x)$ and $z(x)$ is within the limits of one. It can be found that the moving, curved interface is straightened and immobilized in the new transformed coordinate system.

Then equation (3) and (5) can be written in other forms as

$$\rho C_p\left(\frac{\partial T}{\partial t} + u\frac{\partial T}{\partial x}\right) = \frac{\lambda}{\delta^2(x)y}\frac{\partial T}{\partial y} + \frac{\lambda}{\delta^2(x)}\frac{\partial^2 T}{\partial y^2} + \eta\dot{\gamma}^2 \quad (12)$$

$$\rho C_p\frac{\partial T}{\partial t} = \frac{\lambda}{[\delta(x) + g(x)z]g(x)}\cdot\frac{\partial T}{\partial z} + \frac{\lambda}{g^2(x)}\frac{\partial^2 T}{\partial z^2} \quad (13)$$

The alternating direction implicit form[6, 7] for equation (2) may be written as

$$\rho C_p\left|\frac{T_{i,j}^{K+1/2} - T_{i,j}^{K}}{(\Delta t/2)} + u_{i,j}^{K}\frac{T_{i,j}^{K+1/2} - T_{i-1,j}^{K+1/2}}{\Delta x}\right|_l = \left|\frac{\lambda}{\delta^2(x)\Delta yj}\cdot\frac{T_{i,j+1}^{K} - T_{i,j-1}^{K}}{2\Delta y} + \frac{\lambda}{\delta^2(x)}\frac{T_{i,j+1}^{K} - 2T_{i,j}^{K} + T_{i,j-1}^{K}}{(\Delta y)^2} + (\eta\dot{\gamma}_r^2)_{i,j}^{K}\right|_l \quad (14(a))$$

$$\rho C_p\left|\frac{T_{i,j}^{K+1} - T_{i,j}^{K+1/2}}{(\Delta t/2)} + u_{i,j}^{K+1/2}\frac{T_{i,j}^{K+1/2} - T_{i-1,j}^{K+1/2}}{\Delta x}\right|_l = \left|\frac{\lambda}{\delta^2(x)\Delta yj}\cdot\frac{T_{i,j+1}^{K+1} - T_{i,j-1}^{K+1}}{2\Delta y} + \frac{\lambda}{\delta^2(x)}\frac{T_{i,j+1}^{K+1} - 2T_{i,j}^{K+1} + T_{i,j-1}^{K+1}}{(\Delta y)^2} + (\eta\dot{\gamma}^2)_{i,j}^{K+1/2}\right|_l \quad (14(b))$$

where subscript l represents liquid. Thus two equations were derived, one for heat flow in the x direction which was solved for the time step K to $K + 1/2$, another one for heat flow in the y direction for the time step $K + 1/2$ to $K + 1$. The implicit finite difference formulation[9] of equation (3) is

$$\rho C_p \left| \frac{T_{i,j}^{K+1/2} - T_{i,j}^{K}}{\Delta t} \right|_s^a = \left| \frac{\lambda}{(\delta(x) + g(x)\Delta zj)g(x)} \cdot \frac{T_{i,j+1}^{K+1} - T_{i,j-1}^{K+1}}{2\Delta z} + \frac{\lambda}{g^2(x)} \cdot \frac{T_{i,j+1}^{k+1} - 2T_{i,j}^{K+1} + T_{i,j-1}^{K+1}}{(\Delta z)^2} \right|_s \quad (15)$$

where subscript s represents solid.

The TDMA method[7] was used to solve the above equations because tridiagonal matrices involved. As the moving solid/liquid boundary is not known beforehand, a trial-and-error method[8] was applied to guess and correct the location of the interface at any given time:

$$\begin{cases} \delta(x) + g(x)\varepsilon_1 \Rightarrow \delta(x) \\ \text{when } \left| \frac{\partial T}{\partial r} \right|_{r=\delta(x),\, t} > \left| \frac{\partial T}{\partial r} \right|_{r=\delta(x),\, s} \\ \delta(x) - g(x)\varepsilon_2 \Rightarrow \delta(x) \\ \text{when } \left| \frac{\partial T}{\partial r} \right|_{r=\delta(x),\, t} < \left| \frac{\partial T}{\partial r} \right|_{r=\delta(x),\, s} \end{cases} \quad (16)$$

where ε_1 and ε_2 are predetermined constants whose values are usually taken to be 0.01 ~ 0.001. The correcting procedure would be repeated untill the guessing boundary location converge to be within a predetermined small tolerance.

A C++ computer simulation program was developed which is capable of modeling the mold filling process of the feedstock melt with solidification in powder injection molding. Generally, thirty minutes to three hours are needed to finish the whole computing procedure on a pentium 133 personal computer, depending on the physical characteristics of the feedstock and the machine parameters setting.

4 RESULTS AND DISCUSSION

In order to examine the effects of process parameters on the thickness of frozen layer during the molding stage, a feedstock was prepared and tested. The mixture was made of Fe-2% Ni and a wax-polymer binder with the solid loading being 58%. The primary binder was composed of 79% (mass fraction) paraffin wax (PW), 10% high density polyethylene (HDPE), 10% polyethylene vinyl acetate (EVA) and 1% stearic acid (SA). The properties of the feedstock is listed in Table 1. The melting point of PW was taken as the freezing temperature as PW was the dominant component of the binder. The length and radius of the die cavity are 6.0 cm and 0.35 cm respectively.

Table 1 Material properties of the mixture[9]

ρ/(kg·m^{-3})	C_p/(J·kg^{-1}·K^{-1})	n	T_a/K
4 850	847	0.35	2 886
m_0/(Pa·s^n)	λ/(W·m^{-1}·K^{-1})	T_s/K	
5.71	2.24	330	

Fig. 2 illustrates how the relative thickness $(g(x)/R)$ of frozen layer at x = 1.2 cm changes with time during the filling stage. It can be concluded that the frozen layer grows rapidly at the time it just formed but the growth rate decreases with time. For a constant inlet rate and die wall temperature, the solid layer thickness is dominated by viscous heat dissipation ($\eta\dot{\gamma}^2$), heat conduction in the radial direction and heat convection in the axial direction. The heat conducted from the upstream and the heat generated by viscous dissipation in the fluid region should be balanced by the heat conducted into the solid phase. When the flow front approaches any location in the die, a very thin "skin" would forms on the wall. The thickness of this "skin"

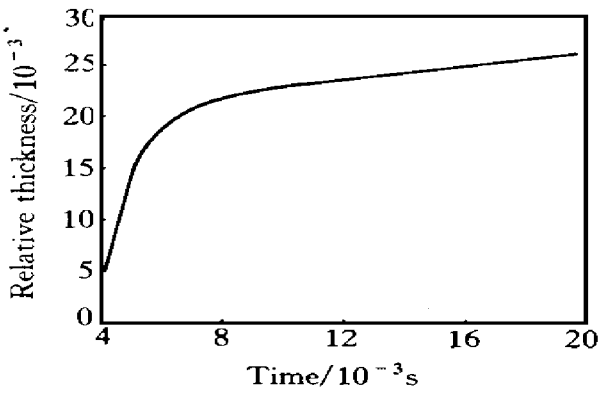

Fig. 2 Relative thickness of solid layer at x = 1.2 cm with filling time (T_0 = 400 K, T_w = 300 K, Q = 120 cm^3/s)

increases quickly because the thermal convection and viscous dissipation are not large enough to compensate the thermal conduction at this time. One might expect that the viscous heat dissipation would finally be balanced by the radial heat conduction in the solid region, so that the solid layer thickness would reach an asymptotic value if the mold be adequately long.

Fig. 3 presents the effect of volume flow rate on the frozen layer profiles when the die were wholly filled. It is evident that the thickness decreases as volume flow rate increases. Shorter residence time, larger viscous heat dissipation and poorer conduction resulting from high volume flow rate would result in a thinner frozen layer. However, as shown in Fig. 3, it can be seen that the difference of solid layer thickness along the flow direction become smaller when the injection flow rate is enough high.

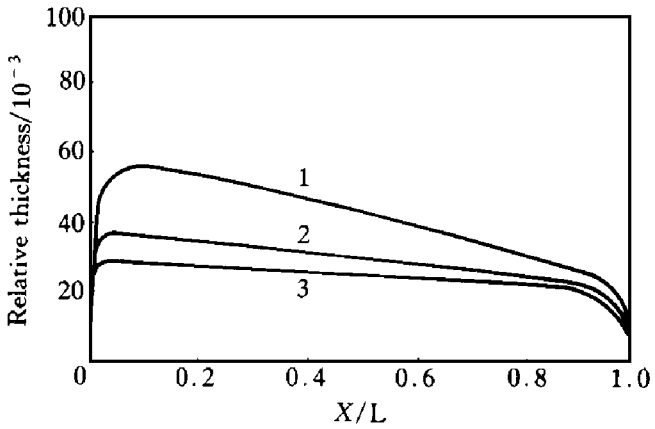

Fig. 3 Solid layer profiles for different flow rates
(1 —Q= 20 cm^3/s; 2 —Q= 50 cm^3/s; 3 —Q= 100 cm^3/s; T_0= 400 K, T_w= 300 K)

Fig. 4 shows the frozen layer profiles at the time the mold being wholly filled for different die wall temperatures (T_w). Apparently, the skin thickness is significantly influenced by T_w. This is because the solid layer thickness is much smaller than the radius of mold cavity thus a little change of wall temperature would dramatically affect the temperature gradient in the solid phase, which subsequently influence the volume of heat conducted into the skin. The higher the mold temperature is, the poorer the thermal conduction might be and so that the thinner the frozen layer generates in order to satisfy the energy balance at the solid/liquid interface.

The effect of injection temperature on the profiles of the skin is presented in Fig. 5. The difference in frozen layer thickness caused by inlet temeprature is not so pronounced as that of wall temperature. Enhancing of the thermal conduction by a higher inlet temperature would be partly compensated by the decreasing of viscous heat dissipation because of the temperature dependent rheological behavior(See equation(1)).

As shown in Fig. 6, the predicting inlet

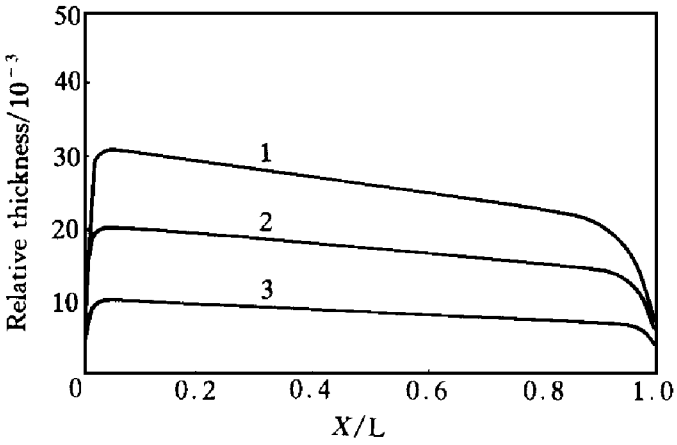

Fig. 4 Solid layer profiles for different mold wall temperatures
(T_0= 400 K, Q= 80 cm^3/s)
1 —T_w= 300 K; 2 —310 K; T_w= 320 K

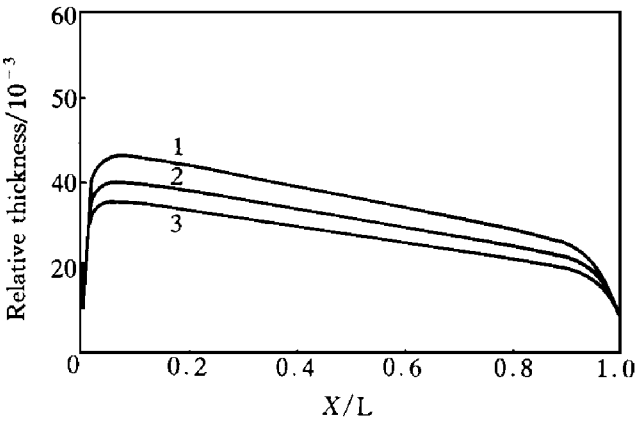

Fig. 5 Solid layer profiles when the mold being wholly filled for different injection temperatures
(T_w= 300 K, Q= 40 cm^3/s)
1 —T_0= 390 K; 2 —T_0= 400 K, 3 —T_0= 410 K

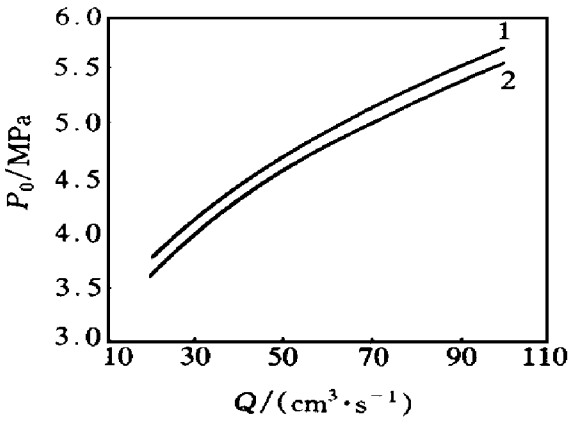

Fig. 6 Effect of volume flow rate on the inlet pressure
(T_0= 440 K, T_w= 300 K)
1 —solidification included;
2 —solidification excluded

pressure at the end of filling stage for the situation that solidification was considered were compared with that of no solidification included. In general, due to the existence of solid layer, the melt flow passage is narrow down so that a larger injection pressure is required. The effect of solidification is closely connected to the accuracy for mold design because improper tool design such as wrong gate location might cause serious solidification of the melt, which subsequently inhibits the filling process and even results in short-shot or other serious molding defects.

REFERENCES

1 Randall M G. Metal Powder Industries Federation (MPIF), Princeton, NJ, 1991.
2 Zhang H, German R M, Hens K F and Lee D. Advances in Powder Metallurgy, Vol. 3, MPIF, American Powder Metallurgy Institute(APMI), 1990.
3 John Crank. Free and Moving Bondary Problems. Oxford: Clarendon Press, 1984.
4 Chen B S and Liu W H. Polymer Engineering and Science, 1989, 29(15): .
5 Ling C, Yang M and Chen S J. Polymer Engineering and Science, 1992, 32(1): .
6 Hunt K N and Evans J R G. Journal of Materials Sciences, 1991, 20(2).
7 Crochet M J, Davies A R, Watters K. Amsterdam: Elsevier Science Publishers, B. V., 1984.
8 Hongsheng Yue. Master Thesis, (in Chinese). Changsha: Central South University of Technology, 1997.
9 Zhu Lei. Master Thesis, (in Chinese). Changsha: Central South University of Technology, 1998.

(Edited by Zhu Zhongguo)